

COVER SHEET

Title: *Component-Based Element of Beam Local Buckling Adjacent to Connections in Fire*

Authors: Guan Quan
Shan-Shan Huang
Ian Burgess

ABSTRACT

An analytical model based on the yield line mechanism [1] has been proposed by the authors to predict the beam-web shear buckling and bottom-flange buckling in fire. This paper described the development of a component-based element considering both buckling phenomena at the beam-ends, based on this analytical model. The component-based buckling element consists of top springs and bottom springs, all of which are capable of dealing with loading-unloading-reloading cycles. This new component-based element has been implemented into the software *Vulcan*, adjacent to the existing component-based connection element. An example case using a single-span beam has been analysed in *Vulcan*. The modelling results have been validated against finite element modelling using *ABAQUS*, indicating that the newly developed component-based buckling element is of good accuracy to reflect the behaviour of local buckling phenomena. Comparison of the structural responses of the beams with and without the buckling element in *Vulcan* has been carried out. This comparison shows that with and without the buckling element does make a difference in the modelling results. This indicates the potential effects of the local buckling at beam ends on the connected joints and columns and on the entire frames at elevated temperatures.

Keywords: Component-based Model, Shear Buckling, Bottom-flange Buckling, Fire

Guan Quan, Department of Civil and Structural Engineering, University of Sheffield, Sir Frederick Mappin Building, Mappin Street, Sheffield S1 3JD, United Kingdom.
Shan-shan Huang, Lecturer, Department of Civil and Structural Engineering, University of Sheffield, Sir Frederick Mappin Building, Mappin Street, Sheffield S1 3JD, United Kingdom.
Ian Burgess, Professor, Department of Civil and Structural Engineering, University of Sheffield, Sir Frederick Mappin Building, Mappin Street, Sheffield S1 3JD, United Kingdom.

INTRODUCTION

The investigation of the collapse of “7 World Trade” as part of the events of 11 September 2001 in the New York City [2] indicated that the connections are among the most vulnerable elements of steel-framed or composite buildings, and their characteristics can determine the survivability of such buildings in extreme scenarios such as fire. In this case total collapse of the building was triggered by the fracture of beam-to-column connections caused largely by thermal expansion of long-span beams. This emphasized the importance of investigating the complex mechanisms through which forces are transferred from the adjacent parts of a structure to the connections under fire conditions.

The Cardington fire tests in 1995-96 [3] provided ample evidence that both shear buckling of beam webs and beam bottom-flange buckling, near to the ends of steel beams (Figure 1), are very prevalent under fire conditions. Both of these phenomena could affect the force distribution at the adjacent column-face connection bolt rows, and therefore the sequence of fracture of components. However, there is a distinct lack of practical research investigating the post-buckling behaviour of beams of Classes 1 and 2 adjacent to connections at elevated temperatures.



Figure 1. Flange-buckling and beam-web shear buckling in combination [3]

The component-based method is a practical approach to carry out structural performance-based analysis with reasonable simplified assumptions under fire conditions. The finite element software *Vucan* [4] was developed by the Fire Engineering Research Group at the University of Sheffield. The component-based connection element has already been included in this software, which enables *Vulcan* to be time saving, compared with other finite element software such as *ABAQUS* and *DIANA*, etc. These features allow engineers to conduct three-dimensional structural robustness assessments under fire conditions.

In this study, the proposed component-based buckling elements have been implemented at both ends of the beam, adjacent to the existing connection elements. The buckling phenomena considered include both the flange-buckling and beam-web shear buckling. Therefore, the buckling element is composed of two parts: flange-buckling element and beam-web shear buckling element. The bottom-flange buckling element is represented by top and bottom components, which will affect the rotation of the whole beam-end. The length of the flange-buckling element is ‘0’. The shear buckling behaviour has been implemented in the existing beam element adjacent to the flange-buckling element by revising its shear modulus in the post-buckling stage to

incorporate the shear buckling behaviour of the beam web, but not changing the original beam curvature. The component-based buckling element is illustrated in Figure 2.

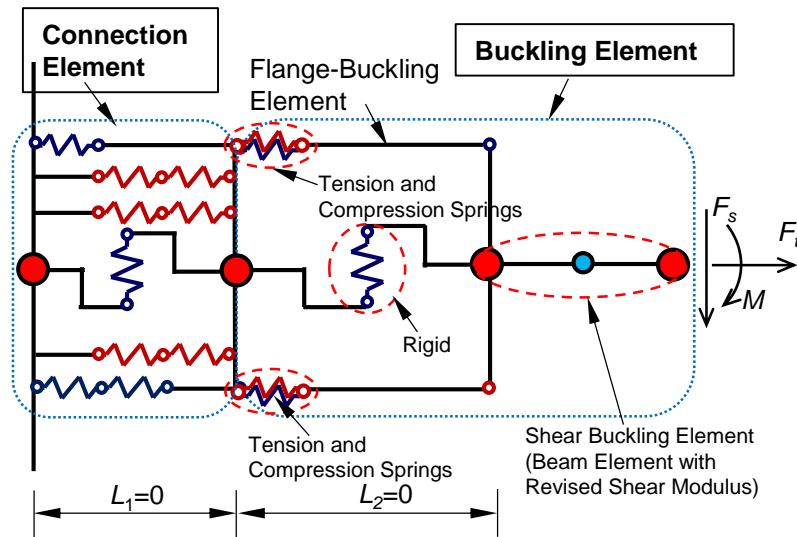


Figure 2. Component-based connections and buckling elements

The flange-buckling element is composed of four nonlinear horizontal springs at the flange positions. Two springs, one tension and one compression, are located at the same position at each flange, providing the resistance of the flanges. For the two springs at the same location, which spring is activated depends on the direction of the spring force; the tensile spring is activated only when the spring is subject to tension and it is switched off and the compression spring becomes active when the spring force is compressive.

1. DEVELOPMENT OF THE COMPONENT-BASED FLANGE-BUCKLING ELEMENT

During the course of fire, the buckling zones can experience high material nonlinearity, and complex combinations of forces caused by the restraints to thermal expansion and to the beam elongation due to beam deflection. These forces will be resisted by the horizontal springs on the flanges (one at each flange). These springs in the buckling element could be subjected either compression or tension at different stages of loading/heating. For example, the bottom spring could be in compression during the heating up, and in tension at the catenary-tension stage. Therefore, it is essential to establish a robust loading-unloading-reloading approach to deal with displacement reversal at both constant and changing temperatures.

1.1 Loading and Unloading of the Flange-Buckling Element at Ambient Temperature

According to the analytical model [1], the schematic characteristics of the compression spring on the buckling flange (assuming it is the bottom flange hereafter), is shown in Figure 3 (a). The characteristics of the compression spring can be divided into three stages: pre-buckling, plateau and post-buckling. The pre-buckling stage ends when the compressive force within the spring reaches F_r , which is the axial force when the bottom half of the I-section yields (Figure 3 (b)). The shape of the curved line in the pre-buckling stage is based on the high-temperature constitutive model of steel given in EC3 Part 1-2 [5].

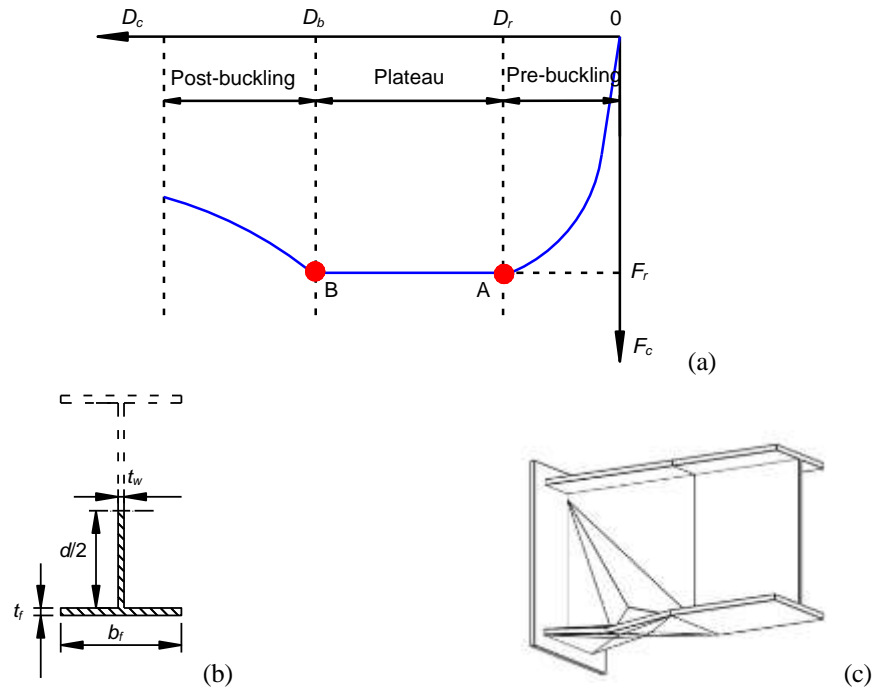


Figure 3. Schematic characteristics of the compression spring on the buckling flange

In this paper, the Masing Rule [6] was applied to each individual spring, through the whole loading-unloading-reloading procedure (including pre-buckling, plateau and post-buckling stages) subject to both steady-state and transient heating.

At ambient temperature, the component characteristics of a spring can be represented by the combination of a skeleton (loading) curve and a hysteresis (unloading) curve. A schematic illustration of the Masing Rule is shown in Figure 4. The hysteresis curve is the skeleton curve scaled by a factor of two and rotated by 180° .

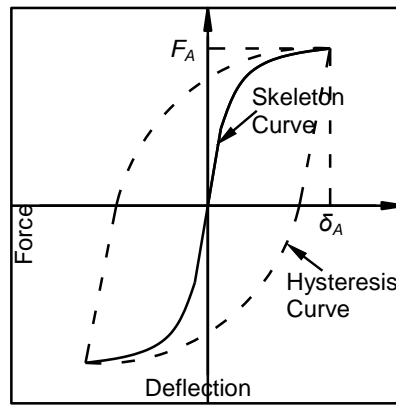


Figure 4. A schematic illustration of the Masing Rule at ambient temperature

The characteristics of the tension spring for the initial loading are similar to that of the compression spring without the post-buckling phase (Figure 5). The unloading procedure follows the same rules as for the compression spring, as described above.

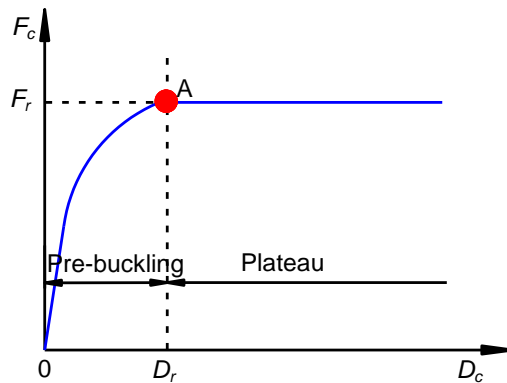


Figure 5. Schematic characteristics of the tension spring

1.2 Loading and Unloading of the Flange-Buckling Element at Elevated Temperatures

At elevated temperatures, the force-displacement characteristic of the springs is temperature-dependent. When temperature changes, it is assumed that the coordinate of the reference point (the point where the unloading path hit the horizontal axis) remains unchanged. The new unloading path will still be linear and follows the initial slope of the force-displacement relationship of the new temperature and so the intersection point (where unloading initiates) relocates. Taking the compression spring in plateau stage as an example, Figure 6 shows the equilibrium stages when temperature changes on this spring.

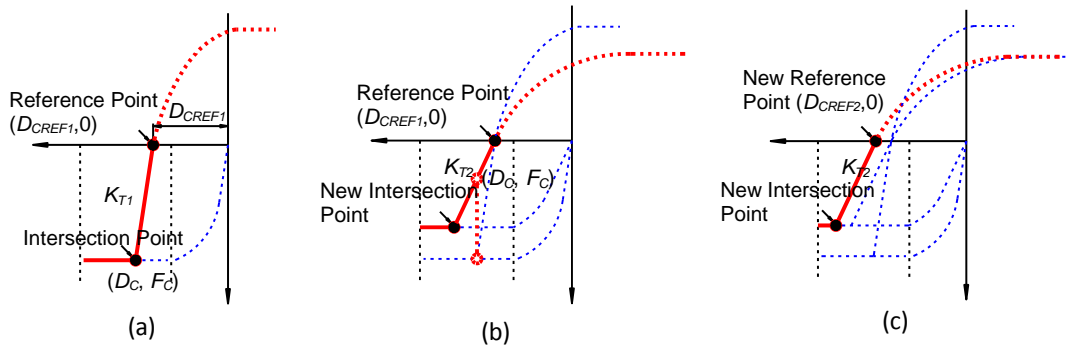


Figure 6. The loading-unloading-reloading loops at different temperatures: (a) at temperature step T_1 (b) during the transition from T_1 to T_2 (c) at temperature step T_2 ($T_2 > T_1$)

The initial stage of the compression spring at temperature T_1 is shown in Figure 6(a). The spring deformation at the reference point can be calculated using,

$$D_{CREF} = D_C - F_C / K_{T1} \quad (1)$$

When temperature elevates to T_2 , the reference point remains unmoved, while the new intersection point can be found using the new initial elastic stiffness K_{T2} at T_2 . The deflection at the new intersection point is,

$$D_{INTER} = D_{CREF} + F_{r2} / K_{T2} \quad (2)$$

When the spring is further loaded at the same temperature (e.g. T_2), the intersection point will be renewed as the spring displacement increase and the reference point will also be renewed accordingly, as shown in Figure 6(c).

2. RESULTS

2.1 Verification of the ABAQUS Model

In order to verify the proposed *Vulcan* buckling element, an example beam was modelled using both *Vulcan* and *ABAQUS*. *Vulcan*'s beam element is actually a wire element and the beam ends are simulated by the new buckling elements. In order to allow comparison, the *ABAQUS* model also consists of three parts: two beam ends modelled by shell elements and the rest of the beam simulated using wire elements, as shown in Figure 7(a). In order to examine the sensitivity of the modelling results to the element types adopted, another *ABAQUS* model (Figure 7(b)) with only wire element was built. The two *ABAQUS* models (one using shell elements to model the beam ends and using wire elements to model the rest of the beam; one modelling the entire beam with wire elements) are expected to lead to identical modelling results. The beam section is UB356x171x51 and it is 3 m long. It is short enough to avoid bottom-flange buckling; it is of full axial and out-of-plane restraints, therefore, no beam-web

shear buckling is allowed. The beam is loaded with uniformly distributed load 40N/mm, and heated by the ISO834 Standard Fire [7] up to 700°C. The two *ABAQUS* models result in exactly the same deflection and axial force, as expected (Figure 7(c)).

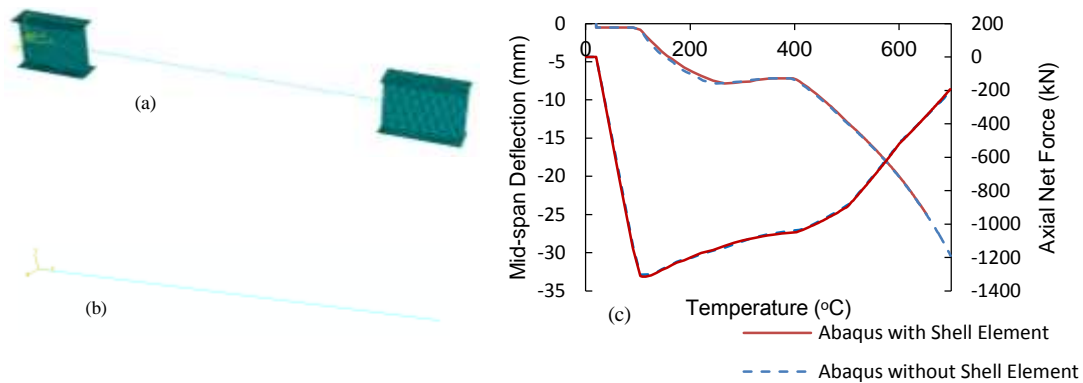


Figure 7. Comparison of *ABAQUS* models: (a) *ABAQUS* image of the 3m beam with shell elements; (b) *ABAQUS* image of the 3m beam with beam elements only; (c) Comparison of the *ABAQUS* results.

2.2 *Vulcan* vs. *ABAQUS*

In order to verify the component-based buckling element, an isolated beam with buckling elements at its ends and wire elements representing the rest of the beam modelled, as shown in Figure 8. The beam section is UB356x171x51. The beam is with full axial and out-of-plane restraints. The beam was initially loaded with uniformly distributed load 40N/mm, and subsequently heated by the ISO834 Standard Fire up to 700°C. The material properties of the steel given in EC3 [5] were adopted.

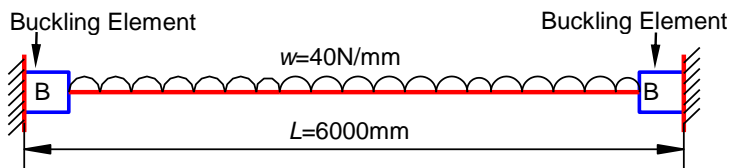


Figure 8. Isolated beam with buckling elements

Figure 9 plots the development of the mid-span vertical deflection with temperature, given by the *ABAQUS* and *Vulcan* models with and without the beam-end shell or buckling elements. It can be seen that, the deflections of the *ABAQUS* and *Vulcan* models with only beam elements compare well; the discrepancy between the two software is because they use different types of wire elements with different shape functions. The *ABAQUS* model with shell elements, which allows the consideration of buckling at the beam ends, experienced a larger mid-span deflection due to beam-end shear buckling and bottom-flange buckling; the *Vulcan* model with the buckling elements is also able to capture the buckling characteristics, and is able to account for the additional deflection caused by beam-end buckling. Figure 9 shows that the deflections of these two models agree with each other. The *Vulcan* model with the

buckling elements failed at around 590°C when both the top and bottom flanges yield without stress hardening, whereas the other three models failed at higher temperatures, because the former uses only two springs to represent the whole beam section which could lead to a slightly early failure compared to the other three models with continuous cross-section at the beam ends.

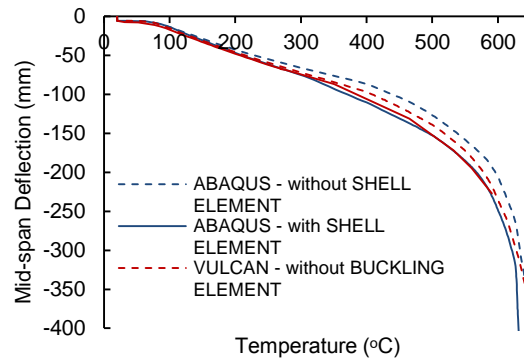


Figure 9. Temperature-Mid-span Deflection Relationship

CONCLUSION

In this paper, the development of a component-based buckling element, including beam-web shear buckling and bottom-flange buckling has been developed, based on a proposed analytical model. The bottom-flange buckling phenomenon is simulated using two top springs and two bottom springs; each spring is able to deal with loading-unloading-reloading cycles. The beam-web shear buckling phenomenon is considered by modifying the shear modulus of the existing beam element of *Vulcan*. This proposed buckling element has been verified against *ABAQUS* models. A good agreement between the *ABAQUS* and *Vulcan* modelling results indicate that the proposed buckling elements in *Vulcan* are capable of reflecting the influence of the beam-web shear buckling and bottom-flange buckling adjacent to the connections.

REFERENCES

1. Quan G, Huang S-S, Burgess I. 2016. "Component-based model of buckling panels of steel beams at elevated temperatures." *Journal of Constructional Steel Research.*, 118:91-104.
2. Gann RG. 2008. "Final Report on the Collapse of World Trade Center Building 7, Federal Building and Fire Safety Investigation of the World Trade Center Disaster," the National Institute of Standards and Technology (NIST), Gaithersburg, US.
3. Newman G, Robinson JT, Bailey CG. 2001. "Fire safe design: A new approach to multi-storey steel-framed buildings," SCI publication.
4. Huang Z, Burgess IW, Plank RJ. 2003. "Modeling membrane action of concrete slabs in composite buildings in fire. I: Theoretical development." *Journal of Structural Engineering.*, 129:1093-102.
5. CEN. 1993. "Eurocode 3: Design of steel structures—Part 1-2: General rules—Structural fire design," European Committee for Standardization, Brussels.
6. Jayakumar P. 1987. "Modeling and identification in structural dynamics," California Institute of Technology.
7. British Standards Institution BS476. 1987. "Fire Tests on Building Materials and Structures, Part 20: Method for Determination of the Fire Resistance of Elements of Construction," London.